Supporting Information

Water-Dispersible Fluorescent Carbon Dots as Bioimaging Agents and Probes for Hg^{2+} and Cu^{2+} ions

Madhuri Bhatt[a,b], Shreya Bhatt[a,b], Gaurav Vyas[a,b], Ishan H. Raval[a], Soumya Haldar[a,b] and Parimal Paul[a,b]*

[a]*Analytical and Environmental Science Division and Centralized Instrument Facility, CSIR-Central Salt and Marine Chemicals Research Institute, G. B. Marg, Bhavnagar 364002, India.*
[b]*Academy of Scientific and Innovative Research (AcSIR), Ghaziabad- 201002, India.*
Corresponding author: E-mail: ppaul@csmcri.res.in (P. Paul),

Table of Content

Figure No.	Figure Caption	Page No.
Figure S1	AFM image of N-CD, insert: height along Z-axis.	S4
Figure S2	Fluorescence spectral change of N-CD in presence NaCl (0.5 to 5.0 %)	S5
Figure S3	Fluorescence spectral change of N-CD at different pH (pH 1-12) in aqueous media.	S6
Figure S4	Fluorescence spectral change of N-CD in presence of various solvents.	S7
Figure S5	Bar diagram showing change in fluorescence intensity of N-CD at 415 nm upon addition of various metal ions (20 µM)	S8
Figure S6	Fluorescence spectral change of N-CD in presence of Cu^{2+} and Hg^{2+} and after addition of ATP into the solution of N-CD-M^{2+} (Metal:ATP molar ratio is 1:2).	S9
Figure S7	Plot of fluorescence quenching efficiency of N-CD as a function of time with different concentration of Hg^{2+}.	S10

Figure S8	Plot of fluorescence quenching efficiency of N-CD as a function of time with different concentration of Cu^{2+}.	S11
Figure S9	The change in quenching intensity [$(F_0/F)-1$] of N-CD as a function of the concentration of Hg^{2+}.	S12
Figure S10	(a) Fluorescence titration of N-CD upon addition of incremental amount of Cu^{2+} (0.10 μM to 0.18 mM), (b) the change in quenching intensity [$(F_0/F)-1$] as a function of the concentration of Cu^{2+} and (c) its linear portion for calculation of quenching constant and to determine concentration of metal ion in unknown solution.	S13
Figure S11	Bar diagram of competitive selectivity of N-CD towards Hg^{2+} (25 μM). Black bar represents the fluorescence intensity at 415 nm of N-CD. The Purple bar represents the fluorescence intensity at 415 nm of N-CD in the presence of Hg^{2+}. The green bars represent the fluorescence intensity at 415 nm upon the subsequent addition of different cations (50 μM).	S14
Figure S12	Bar diagram of competitive selectivity of N-CD towards Cu^{2+} (25uM). Black bar represents the fluorescence intensity at 415 nm of N-CD. Blue bar represents the fluorescence intensity at 415 nm of N-CD in the presence of Cu^{2+}. The purple bars represent the fluorescence intensity at 415 nm upon the subsequent addition of different cations (50 μM).	S15
Figure S13	(a) Emission decay of N-CD in presence of Cu^{2+}, experimental (dotted curve) and the fitted curve (full line) in aqueous medium and (b) Emission decay of N-CD in presence of Hg^{2+}, experimental (dotted curve) and the fitted curve (full line) in aqueous medium.	S16
Figure S14	Ratios of emission life-time of N-CD with different concentration of (a) Cu^{2+} ion and (b) Hg^{2+} ion.	S17
Figure S15	UV-vis spectra of N-CD, Hg^{2+} and Cu^{2+} solutions with perchlorate anion (50 μM) and N-CD upon addition of Hg^{2+} and Cu^{2+} solutions.	S18
Figure S16	Plot for estimation of Hg^{2+} ion in real samples using the linear segment of the standard curve obtained from fluorescence titration of N-CD using standard solutions of Hg^{2+}.	S19

Figure S17	Plot for estimation of Cu^{2+} ion in real samples using the linear segment of the standard curve obtained from fluorescence titration of N-CD using standard solutions of Cu^{2+}.	S20
Figure S18	Paper strips coated with N-CD, (a) dipped into aqueous solution of different metal ions (5 μM) for five minutes and dried in air (colour change was noted for Cu^{2+} and Hg^{2+}) and (b) a pinch of solid $HgCl_2$ and $CuCl_2$ were kept on the strips and were removed after five minutes (colour change of the spot was noted).	S21
Figure S19	Mortality percentage (%) calculation for N-CD, N-CD-Cu^{2+} and N-CD-Hg^{2+}.	S22
Table S1	Real sample analysis for Hg^{2+} and Cu^{2+} in water using N-CD and ICP-MS.	S23

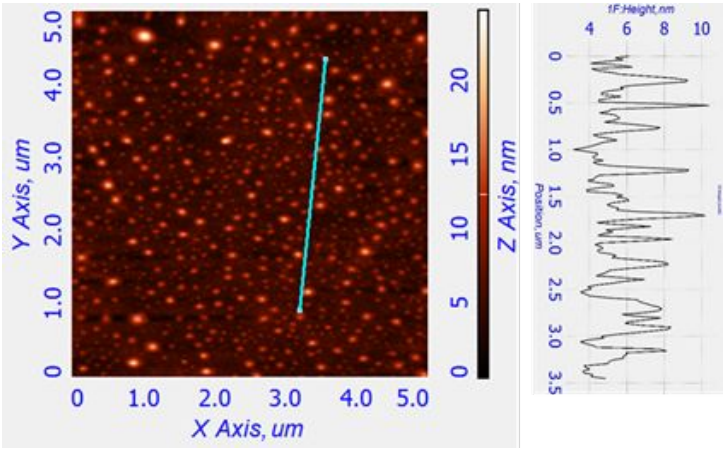

Figure S1. AFM image of N-CD, insert: height along Z-axis.

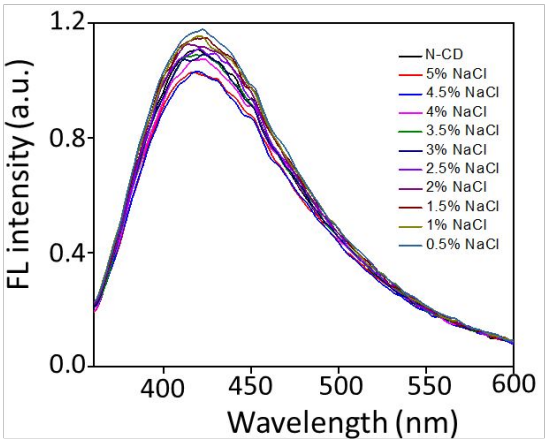

Figure S2. Fluorescence spectral change of N-CD in presence NaCl (0.5 to 5.0 %).

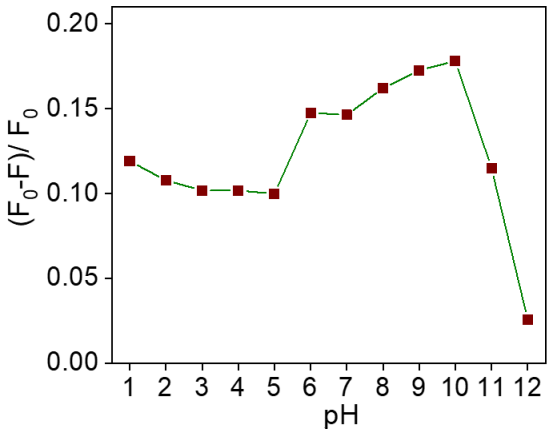

Figure S3. Fluorescence spectral change of N-CD at different pH (pH 1-12) in aqueous media.

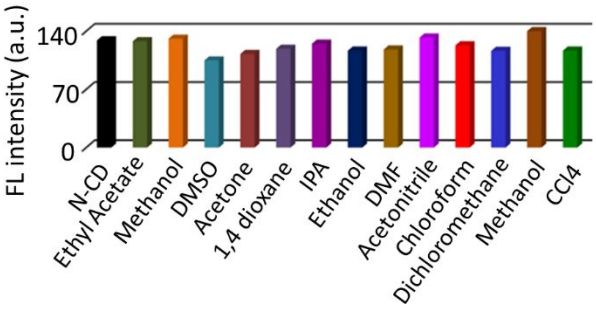

Figure S4. Fluorescence intensity of N-CD in various solvents.

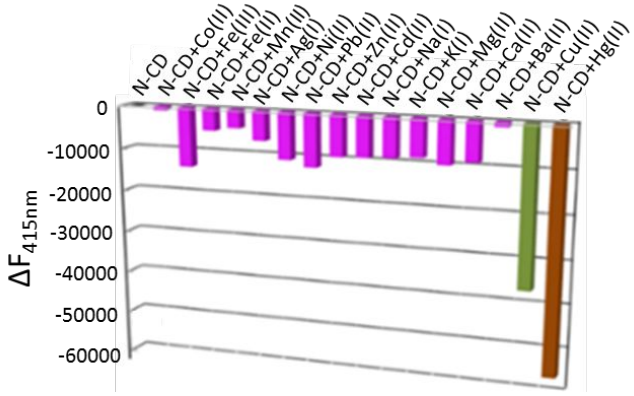

Figure S5. Bar diagram showing change in fluorescence intensity of N-CD at 415 nm upon addition of various metal ions (20 μM).

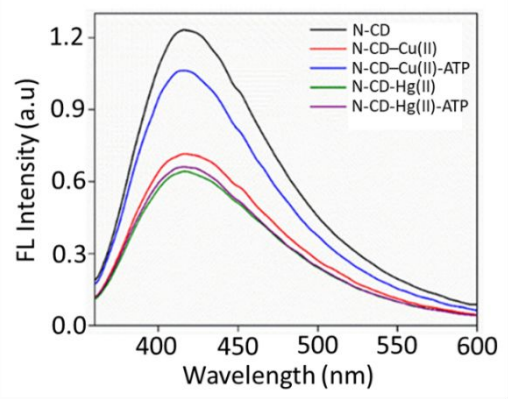

Figure S6. Fluorescence spectral change of N-CD in presence of Cu^{2+} and Hg^{2+} and after addition of ATP into the solution of N-CD-M^{2+} (Metal: ATP molar ratio is 1:2).

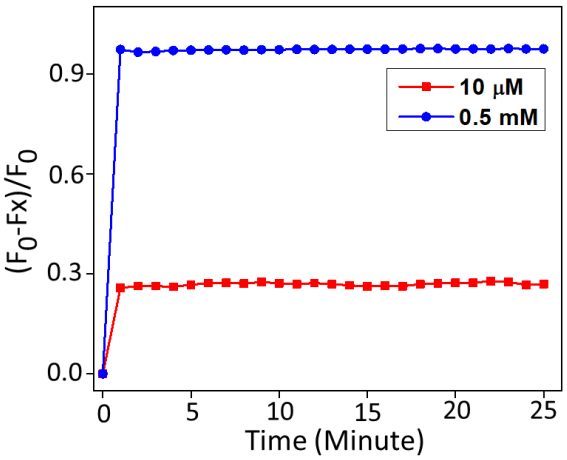

Figure S7. Plot of fluorescence quenching efficiency of N-CD as a function of time with different concentration of Hg^{2+}.

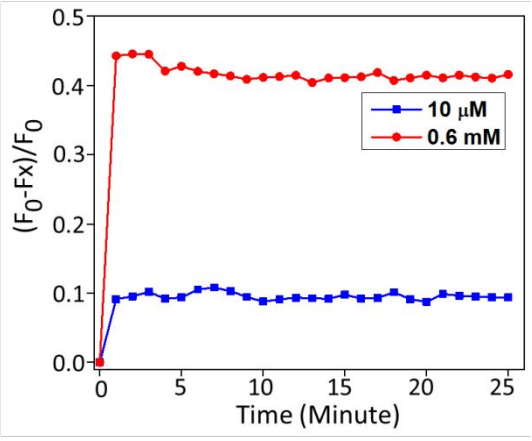

Figure S8. Plot of fluorescence quenching efficiency of N-CD as a function of time with different concentration of Cu^{2+}.

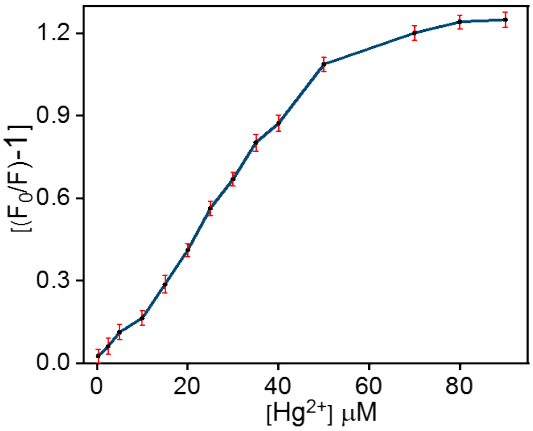

Figure S9. The change in quenching intensity [*(F₀/F)-1*] of N-CD as a function of the concentration of Hg^{2+}.

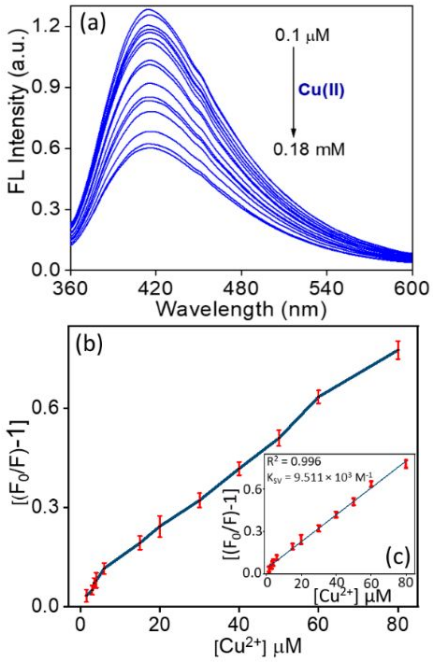

Figure S10. (a) Fluorescence titration of N-CD upon addition of incremental amount of Cu^{2+} (0.10 μM to 0.18 mM), (b) the change in quenching intensity [$(F_0/F)-1$] as a function of the concentration of Cu^{2+} and (c) its linear portion for calculation of quenching constant and to determine concentration of metal ion in unknown solution.

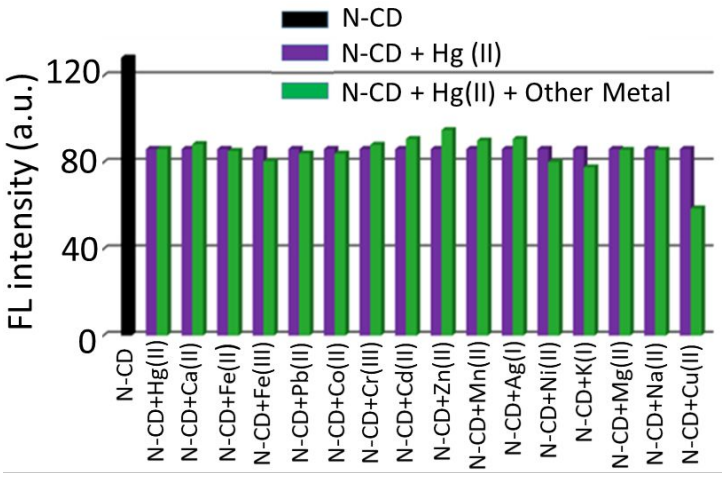

Figure S11. Bar diagram of competitive selectivity of N-CD towards Hg^{2+} (25 μM). Black bar represents the fluorescence intensity at 415 nm of N-CD. The Purple bar represents the fluorescence intensity at 415 nm of N-CD in the presence of Hg^{2+}. The green bars represent the fluorescence intensity at 415 nm upon the subsequent addition of different cations (50 μM).

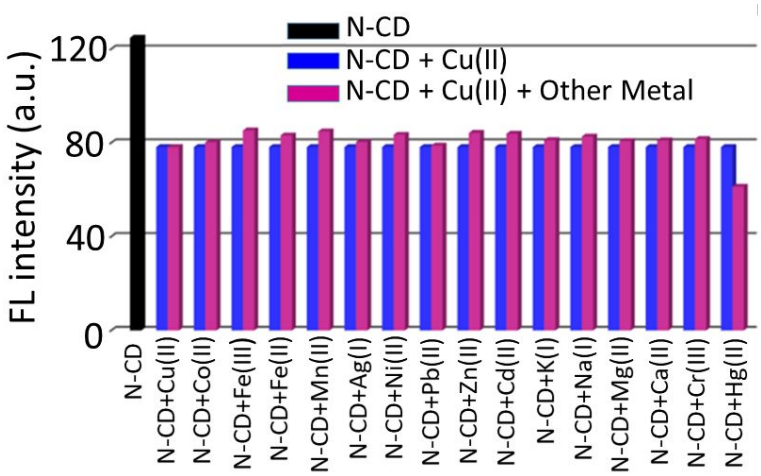

Figure S12. Bar diagram of competitive selectivity of N-CD towards Cu^{2+} (25uM). Black bar represents the fluorescence intensity at 415 nm of N-CD. Blue bar represents the fluorescence intensity at 415 nm of N-CD in the presence of Cu^{2+}. The purple bars represent the fluorescence intensity at 415 nm upon the subsequent addition of different cations (50 μM).

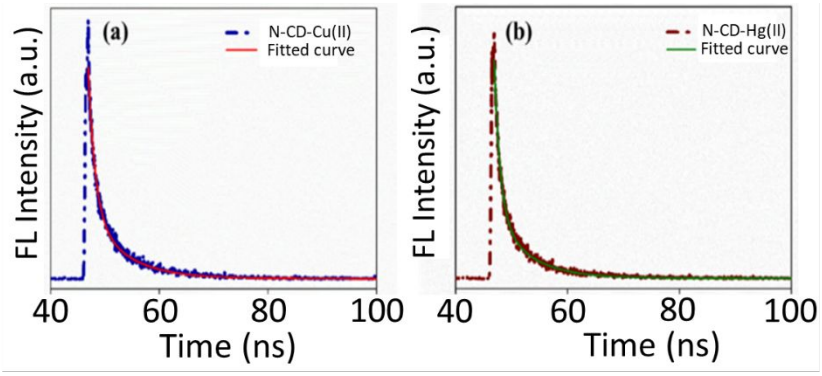

Figure S13. (a) Emission decay of N-CD in presence of Cu^{2+}, experimental (dotted curve) and the fitted curve (full line) in aqueous medium and (b) Emission decay of N-CD in presence of Hg^{2+}, experimental (dotted curve) and the fitted curve (full line) in aqueous medium.

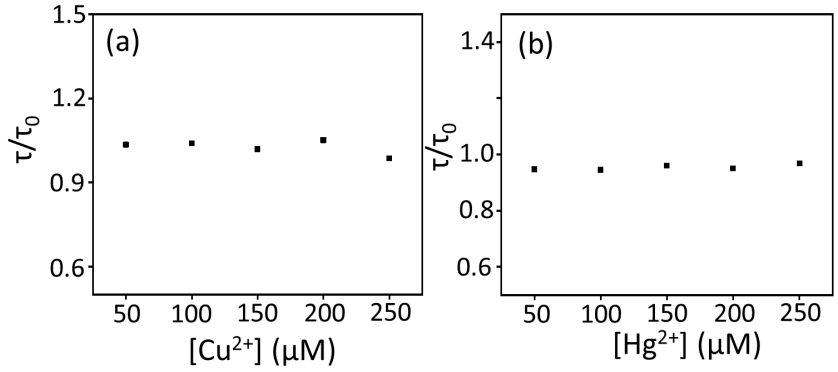

Figure S14. Ratios of emission life-time of N-CD with different concentration of (a) Cu^{2+} ion and (b) Hg^{2+} ion.

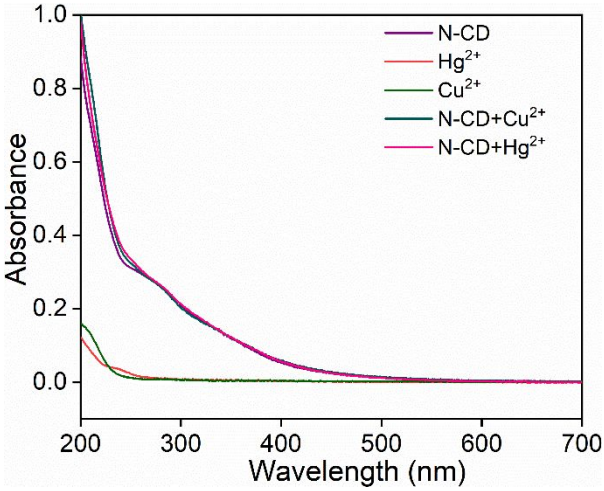

Figure S15. UV-vis spectra of N-CD, Hg^{2+} and Cu^{2+} solutions with perchlorate anion (50 μM) and N-CD upon addition of Hg^{2+} and Cu^{2+} solutions.

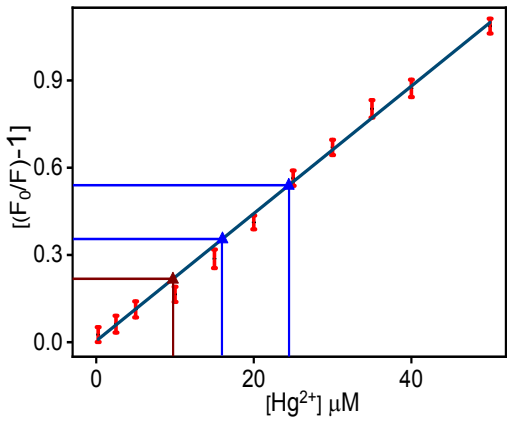

Figure S16**.** Plot for estimation of Hg^{2+} ion in real samples using the linear segment of the standard curve obtained from fluorescence titration of N-CD using standard solutions of Hg^{2+}.

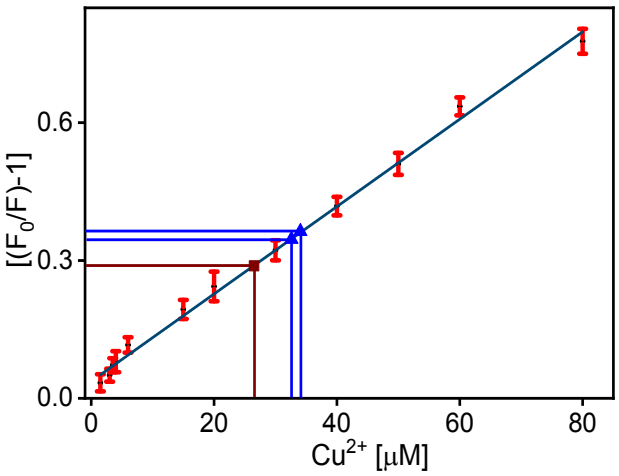

Figure S17. Plot for estimation of Cu^{2+} ion in real samples using the linear segment of the standard curve obtained from fluorescence titration of N-CD using standard solutions of Cu^{2+}.

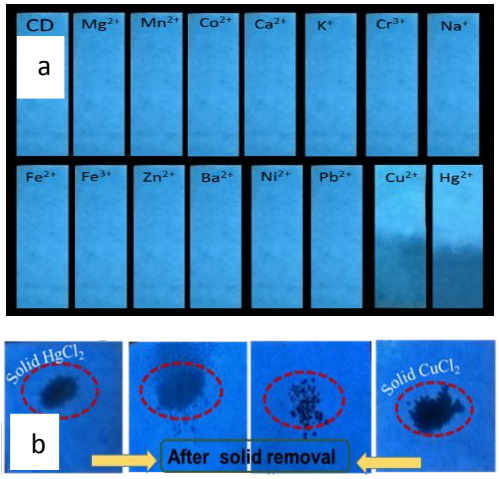

Figure S18. Paper strips coated with N-CD, (a) dipped into aqueous solution of different metal ions (5 μM) for five minutes and dried in air (colour change was noted for Cu^{2+} and Hg^{2+}) and (b) a pinch of solid $HgCl_2$ and $CuCl_2$ were kept on the strips and were removed after five minutes (colour change of the spot was noted).

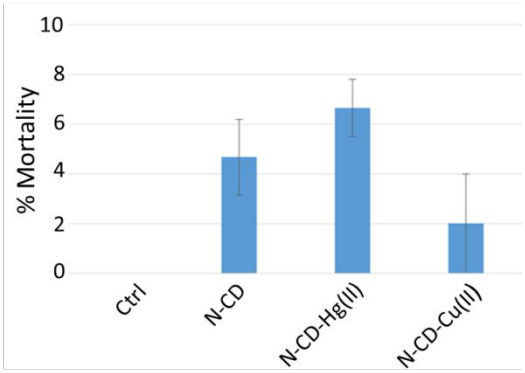

Figure S19. Mortality percentage (%) calculation for N-CD, N-CD-Cu^{2+} and N-CD-Hg^{2+}.

Table S1. Real Sample Analysis for Hg^{2+} and Cu^{2+} in Water Using N-CD and ICP-MS

sample ID	spiked amount (μM)	ICP-MS (μM)	using N-CD (μM)	recovery (%)
		Hg^{2+}		
DW 1	10.00	12.81	10.73	107.3
TW 1	15.00	17.73	16.04	106.9
TW 1	25.00	25.29	24.39	97.5
		Cu^{2+}		
DW 1	25.00	23.68	26.51	106.0
TW 1	30.00	27.38	32.59	108.6
TW 2	35.00	35.25	34.05	97.2

DW = Drinking water, TW = Tap water